System model of an Image Stabilization System

Manuel Carmona[a], José María Gómez[a, b], David Roma[a], Albert Casas[a], Manel López[a], José Bosch[a], Atilà Herms[a], Josep Sabater[a, b], Reiner Volkmer[c], Frank Heidecke[c], Thorsten Maue[c], Eiji Nakai[c], Wolfgang Schmidt[c]

[a]Dept of Electronics, Univ. de Barcelona, Marti i Franquès 1, E08028 Barcelona, Spain; [b]Institut de Ciències del Cosmos, Univ. de Barcelona (IEEC-UB), Martí Franquès 1, E08028 Barcelona, Spain; [c]Kiepenheuer-Institut für Sonnenphysik, Schöneckstraße 6, 79104 Freiburg im Breisgau, Germany

ABSTRACT

The Polarimetric and Helioseismic Imager (PHI) instrument is part of the remote instruments for the ESA Solar Orbiter (SO), which is scheduled to launch in 2017. PHI captures polarimetric images from the Sun to better understand our nearest star, the Sun. A set of images is acquired with different polarizations, and afterwards is processed to extract the Stokes parameters. As Stokes parameters require the subtraction of the image values, in order to get the desired quality it is necessary to have good contrast in the image and very small displacements between them. As a result an Image Stabilization System (ISS) is required. This paper is focused in the behavior and the main characteristics of this system. This ISS is composed of a camera, a tip-tilt mirror and a control system. The camera is based on a STAR1000 sensor that includes a 10 bits resolution high-speed Analog-to-Digital Converter (ADC). The control system includes a Correlation Tracking (CT) algorithm that determines the necessary corrections. The tip-tilt mirror is moved based on this corrections to minimize the effects of the spacecraft (S/C) drift and jitter with respect to the Sun. Due to its stringent requirements, a system model has been developed in order to verify that the required parameters can be satisfied. The results show that the ISS is feasible, although the margins are very small.

Keywords: Solar Orbiter, Polarimetric and Helioseismic Imager, SO/PHI, Image Stabilization System, Correlation Tracking, Space electronics.

1. INTRODUCTION

The Sun's atmosphere and heliosphere represent unique accessible domains of space where fundamental physical processes common to solar, astrophysical and laboratory plasmas can be studied in detail. These phenomena occur under conditions impossible to reproduce on Earth or to study from astronomical distances. The ESA mission Solar Orbiter will provide in-situ measurements that will bring about major breakthroughs in solar and heliospheric physics[1].

To examine the surface by visible light and measure local magnetic fields, Solar Orbiter will carry a high-resolution magnetograph. This instrument is the Polarimetric and Helioseismic Imager (SO/PHI)[2]. PHI will be composed of two telescopes. The High Resolution Telescope (HRT) will image a fraction of the solar disk at a resolution reaching 150 km at perihelion; while the Full Disk Telescope (FDT) will be able to image the full solar disk at all phases of the orbit. The HRT and the FDT will sequentially send light to a Fabry-Perot filtergraph system (~ 100 mÅ spectral resolution) and on to a high resolution APS sensor that will capture the scientific images. This camera is shared for both telescopes. PHI will have its own Image Stabilization System (ISS) for the HRT. This system will include a second camera, with lower resolution and higher frame rate, a Correlation Tracker[3] and a rapid tip-tilt mirror. As the aim of the ISS is to remove the jitter and drift on the scientific images, it has includes a fast control algorithm, able to correct them. Previous Solar missions have implemented an equivalent stabilization system: Luminosity Oscillation Imager (SOHO mission)[4, 5], Guide Telescope (STEREO mission)[6] or the Correlation Tracker (SOLAR B)[7]; in this case, an APS will be used, with larger image size (128x128pixels) at nearly 400fps, searching an attenuation of 10 at 10Hz.

Modeling, Systems Engineering, and Project Management for Astronomy VI,
edited by George Z. Angeli, Philippe Dierickx, Proc. of SPIE Vol. 9150, 91501U
 · doi: 10.1117/12.2054867

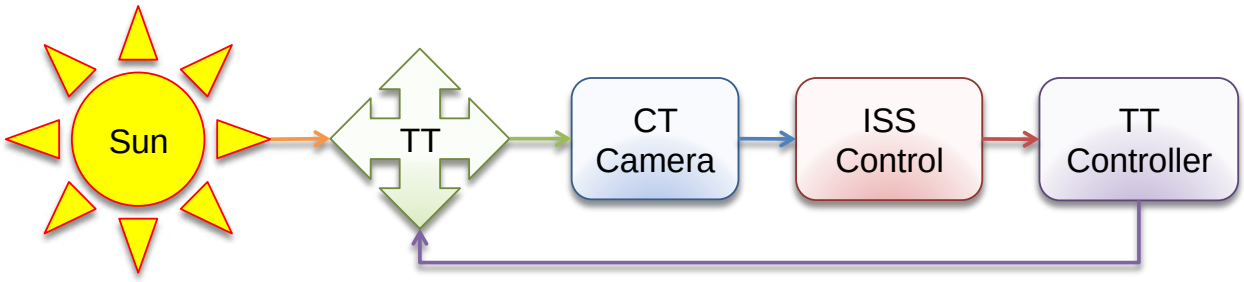

Fig. 1 ISS block diagram.

As shown in Figure 1, the ISS is formed by four main elements: The tip tilt mirror, the camera and finally the ISS control. The Sun light is received by the HRT telescope, and it is reflected by the TT Mirror, which is controlled by the TT Driver. Part of this light is focalized on the CT camera sensor forming an image. This image is sent to the ISS Control algorithm, which compares this image with a reference one. Based on the results, the ISS control gives a signal to the TT Controller, which moves the TT Driver and as a result the TT Mirror. The whole system works in close-loop, allowing a precise control.

2. ISS COMPONENTS

The components described before are distributed between both PHI instrument units:

- Optics Unit (O-Unit): Includes all the optical elements, sensors and its proximity electronics. The TT Mirror and the CT Camera are place in this unit.
- Electronics Unit (E-Unit): Has all the control electronics, including the Digital Processing Unit, where the ISS Control algorithm works, and the TT Controller.

In the following subsections, the different elements are described.

2.1 TT Mirror

The TT Mirror is composed by the M2 mirror of the HRT and a TT Drive, which moves the mirror following the commands given by the ISS Control. The TT Drive is based on the Physical Instrument S-340[8]. This is a tip/tilt platform based on four Piezo-electric Transducer (PZT) stacks that allows movements in two orthogonal axes with a common pivot point (parallel kinematics). On the top platform, the M2 mirror of the HRT is placed. The figure 2 shows the platform block diagram.

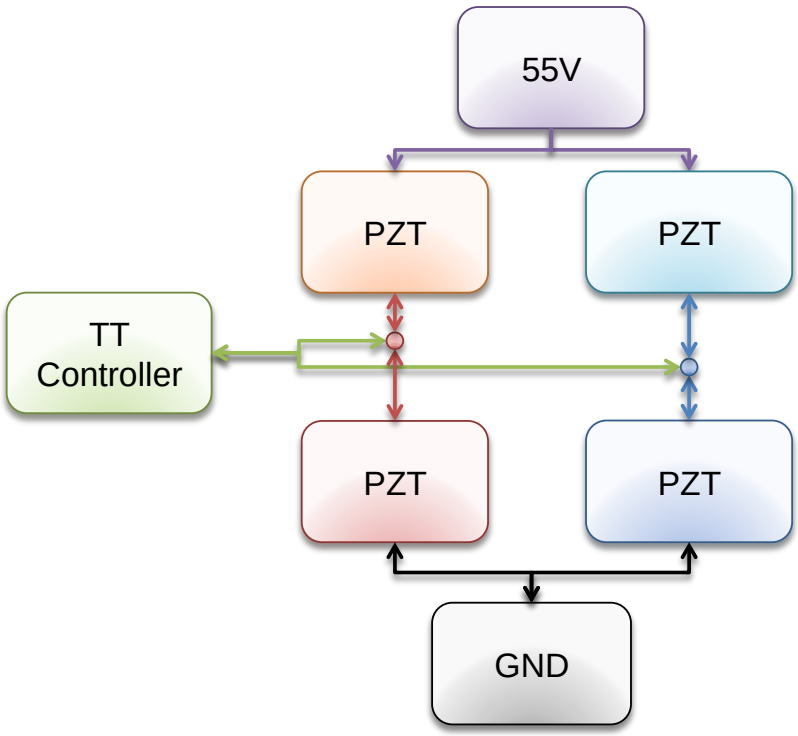

Fig. 2 TT Driver block diagram.

The PZT have reduced hysteresis and only require 55V to reach the required displacements. The platform is controlled through two channels that drive the movement of their respective axis.

2.2 CT Camera

The CT Camera is based on the image sensor STAR1000[9], as it is able to provide a frame rate above 300fps with image sizes of 128x128 pixels. As it has been indicated, the CT Camera is separated from the processing hardware. The first is located in the O-Unit, while the second is in the E-Unit. The interface used is serial. For this reason the front end electronics includes an ADC to digitalize and an FPGA to control the sensor and the ADC, provide the data interface, and manage the housekeeping. The block diagram is shown in Figure 3.

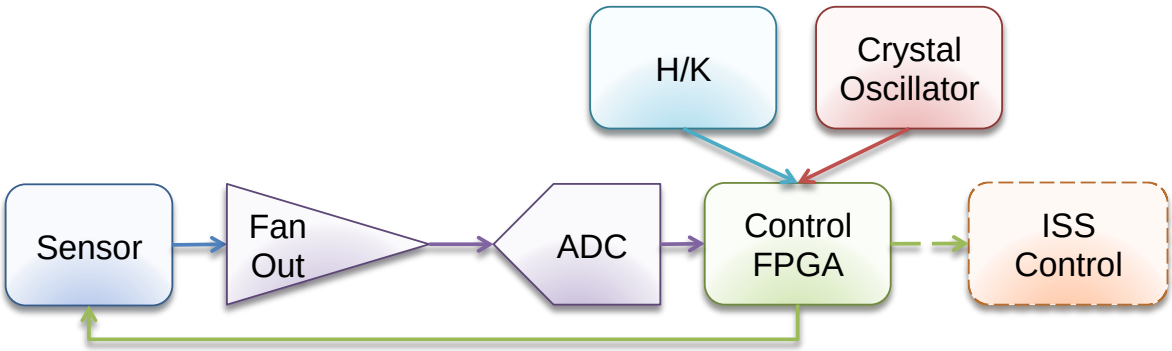

Fig. 3 CT camera block diagram.

The sensor analog output is connected to the ADC through the fan-out amplifier. The Control FPGA is in charge of both, the sensor and the ADC. The captured image is sent through a serial interface to the ISS control algorithm that runs inside the DPU. The circuit also includes a crystal oscillator to synchronize the different elements. One example of the images received by the CT Camera is shown in Figure 4.

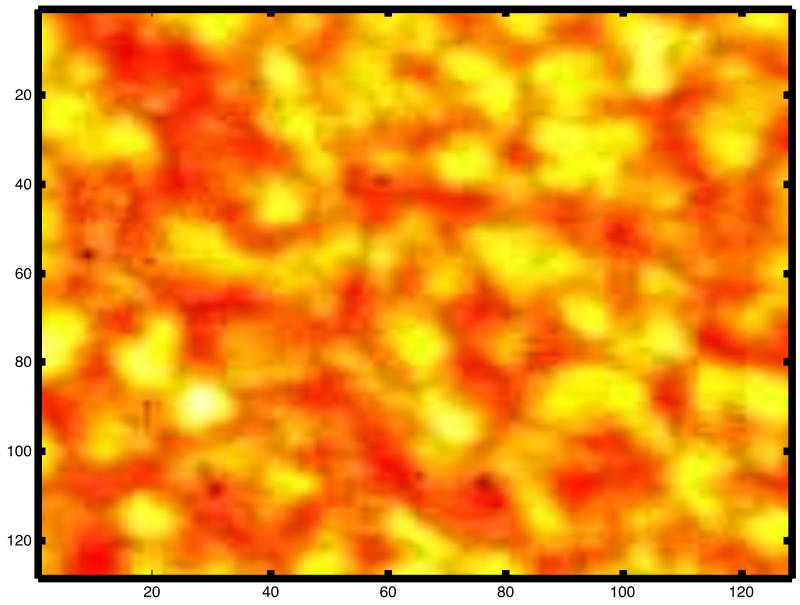

Fig. 4 Example of a CT Camera Image.

Figure 4 shows the Sun granularity. These granules evolve with time, introducing artifacts that have to be taken into account in the ISS Control design.

2.3 TT Controller

The TT Mirror is controlled through the TT Controller. This board includes a dual control amplifier for the two TT Mirror channels. The TT Mirror can also introduce jitter if the control signals are not stable enough. For this reason, a highly stabilized 55V regulator has been included. Taking into account that the load is mainly capacitive, the output stage is based on a current operational amplifier. The block diagram is shown in the Figure 5.

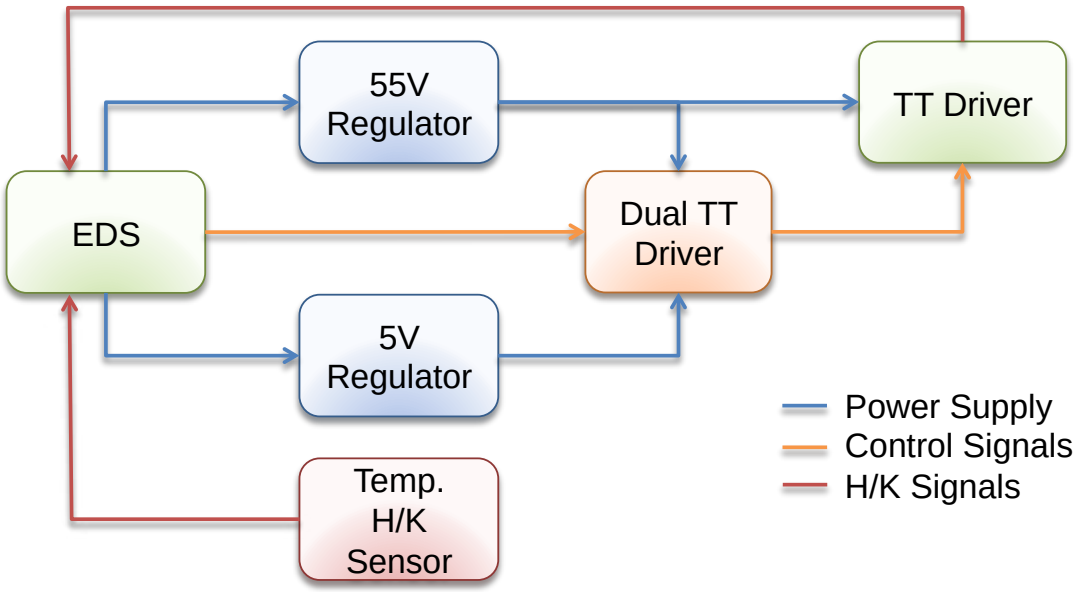

Fig. 5 TT Controller block diagram.

The TT Controller is connected to the ISS Control that runs in the DPU through the E-Unit Electric Distribution System (EDS). The TT Driver is controlled through the amplifier, moving the TT Mirror acordingly. The interface to the DPU

uses the serial one provided by the two DACs (DAC121S101QML[10]) controls the amplifiers. The ISS Control will manage this connection.

2.4 ISS Control

The ISS Control is a firmware that runs inside a Virtex 4 SX55 FPGA[11]. It has two main functions:

- Based on the CT camera images, it determines the image shift with resolution of 1/16th of a pixel and sends the corresponding correction signal to the TT controller.
- Manage the whole Image Stabilization System

The CT algorithm is based on Quadratic Differences[12]. The base QD equation is:

$$QD[k,l] = \sum_{i=0}^{M}\sum_{j=0}^{M}\left(I_n[i+k, j+l] - I_{ref}[i,j]\right)^2 \quad (1)$$

Where I_n is the actual image, while I_{ref} is the image that is used as reference.

The first step needed to apply the correlation algorithm is an image reduction, which corrects the effect of non-idealities of the sensor. A flat-field and dark signal correction is done, using the formula:

$$I_{red}[i,j] = \frac{I_{sensor}[i,j] - D[i,j]}{F[i,j] - D[i,j]} \quad (2)$$

To simplify the calculus, the elements can be rearranged, reducing the calculus to a multiplication and an add operation:

$$\begin{cases} I_{red} &= G[i,j]\cdot I_{sensor}[i,j] + O[i,j] \\ G[i,j] &= \dfrac{1}{F[i,j] - D[i,j]} \\ O[i,j] &= -G[i,j]\cdot D[i,j] \end{cases} \quad (3)$$

The coefficients for the gain (G) and offset (O) have only to be calculated at the beginning of a full operation, as both values will change slowly over time.

Once the image reduction has been done, the QD matrix is calculated using the equation (1). The displacement of the image is given by the difference between the center element and the minimum position. For this reason it is necessary to do a search inside the matrix, to find this minimum value position. This will provide the displacement with pixel resolution.

In our application, the displacement shall be measured with subpixel resolution. For this purpose, it is necessary to make an interpolation around the minimum value, to find the minimum to improve the precision. This interpolation is usually done using the center value (placed in the minimum position) and the eight nearest-neighbors (NN).

The preferred method is to use a paraboloid interpolation. To simplify the calculation, a change of coordinates is made. The pixel that has a minimum AD becomes the position (0,0), and the NN have a coordinate range between -1 and 1. As a consequence, the paraboloid formula becomes:

$$\begin{cases} AD^2(x,y) = a_{20}x^2 + a_{02}y^2 + a_{11}xy + a_{10}x + a_{01}y + a_{00} \\ x \in [-1,1] \\ y \in [-1,1] \end{cases} \quad (4)$$

In this case, the minimum position can be found analytically.

$$\begin{cases} x = \dfrac{a_{01}a_{11} - 2a_{02}a_{10}}{4a_{02}a_{20} - a_{11}^2} \\ y = \dfrac{a_{10}a_{11} - 2a_{20}a_{01}}{4a_{02}a_{20} - a_{11}^2} \end{cases} \quad (5)$$

To obtain the six parameters needed, there are different options. One is to use the quadratic interpolation method (QI). The coefficients become:

$$\begin{cases} a_{10} = \dfrac{1}{2}\left(AD^2_{(1,0)} - AD^2_{(-1,0)}\right) \\ a_{01} = \dfrac{1}{2}\left(AD^2_{(0,1)} - AD^2_{(0,-1)}\right) \\ a_{20} = \dfrac{1}{2}\left(AD^2_{(1,0)} - 2\cdot AD^2_{(0,0)} + AD^2_{(-1,0)}\right) \\ a_{02} = \dfrac{1}{2}\left(AD^2_{(0,1)} - 2\cdot AD^2_{(0,0)} + AD^2_{(0,-1)}\right) \\ a_{11} = \dfrac{1}{4}\left(AD^2_{(1,1)} - AD^2_{(-1,1)} - AD^2_{(1,-1)} + AD^2_{(-1,-1)}\right) \end{cases} \quad (6)$$

The solution is analytical, simplifying its calculations. This result has to be processed to get the final values that shall be sent to the TT Controller.

Taking into account the previous information, there is a major driver that defines the ISS Control architecture, which is the loop performance and stability. This driver depends on the CT Algorithm precision, and the delay introduced by the different elements (camera, algorithm calculation and TT movement).

The maximum allowed delay for the CT Algorithm highly depends on the characteristics of the rest of the elements, for this reason the ISS stability has been analyzed.

3. ISS STABILITY CALCULATION

The stability calculation is based on the system block diagram shown in Figure 6.

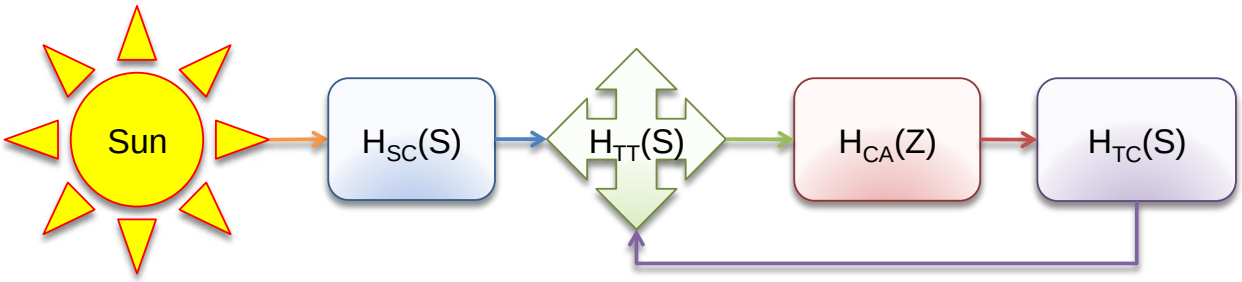

Fig. 6 ISS Control loop diagram.

The control loop elements are:

- H_{SC} is Spacecraft (S/C) transfer function, which introduces the jitter. It is a continuous time function, and can be described using the Laplace transform.
- H_{TT} is the HRT Tip-Tilt transfer function. It works also in the continuous domain and behaves like a second order electro-mechanical filter.
- H_{CA} is the Control Algorithm. It works in the discrete time domain and, as such, it is described using the Z transform.
- H_{TC} is the TT Controller transfer function. Its input is in discrete time, but the whole circuit (the push-pull stage) works in continuous time, so it is also described as a Laplace transform.

As the Control Algorithm is in the discrete domain, we are going to discretize the other transfer functions.

3.1 System transfer function

The first step is determining the system transfer function. This will be done analyzing every one of the loop elements, and finally integrating them in the control loop. The first block is the S/C transfer function. At the present time, this block is unknown, as it is still being designed, but it can modeled as a signal, which will be the pointing position, and a noise, which would be the effect of the jitter. The model is shown in Figure 7.

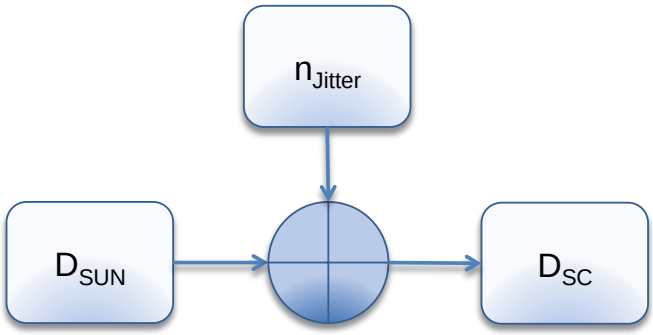

Fig. 7 H_{SC} block diagram.

The image received by PHI has a displacement (D_{SUN}) and a Jitter (n_{Jitter}). In standard conditions, the D_{SUN} has to be 0, while the n_{Jitter} is unknown, as it will depend on many mechanical factors that have to be defined. As a result, the displacement seen by the ISS (D_{SC}) shall be the jitter introduced by the S/C and instruments mechanisms.

The second block can be modeled as shown in Figure 8.

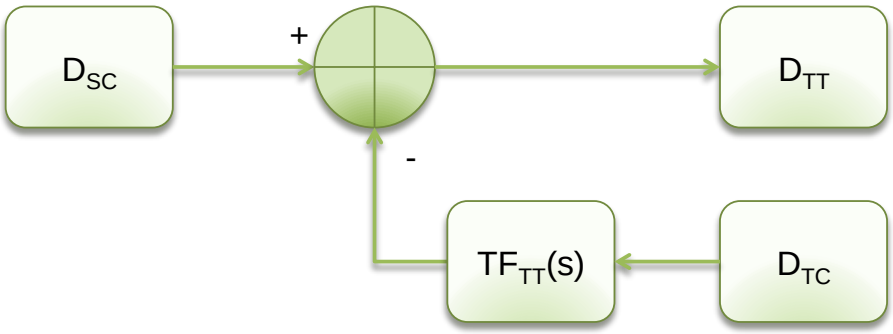

Fig. 8 H_{TT} block diagram.

The TT is controlled by the TT controller displacement signal (D_{TC}). The TT has an electromechanical effect introduced by the Piezo stack and the mechanical structure, which can be modeled by the TT transfer function (TF_{TT}). The resulting movement is subtracted to the S/C displacement, yielding the TT displacement (D_{TT}). As a first approximation, the TT transfer function can be modeled as a second order system:

$$TF_{TT}(s) = \frac{K_{TT}}{\frac{s^2}{\omega_0^2} + 2\xi\frac{s}{\omega_0} + 1} \quad (7)$$

Where K_{TT} is the TT gain, ω_0 is the resonant frequency, and ξ the damping factor.

The Control Algorithm block is shown in Figure 9.

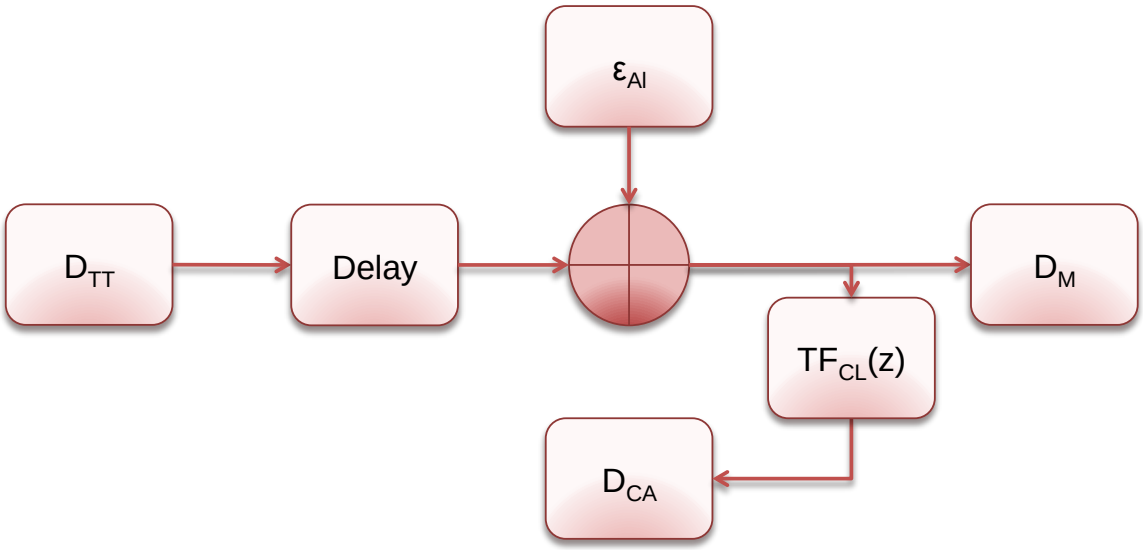

Fig. 9 H_{CA} block diagram.

The image from the CT camera is received, displaced D_{TT}, and after some operations which introduce a Delay, the displacement is measured (D_M) with some error (ε_{AI}). This displacement is filtered applying the Control Loop transfer function (TF_{CL}). The result is the control algorithm calculated distance (D_{CA}), which is the feedback signal.

The block is complex to model, as it works at different frequencies. The main one is the FPGA frequency, which is the fastest. The second is the frame rate, which would be equivalent to a sampling rate. For this reason, we take the frame period as the sampling period (T_s), which is 1/300 fps or 3.3ms.

To model the Control Algorithm block, all the operations inside the block are considered instantaneous. The Delay factor aggregates all the different delays:

- The frame sampling time
- The time necessary to receive the whole image
- The time to calculate the displacement
- The time to calculate the control loop filter
- The time to send the signal to the TT Controller

The total delay is a rational factor of the sampling period, and cannot be easily modelled in the Z domain. For this reason, it is necessary to divide the delay in two contributions, the integer factor of the sampling period and the fractional one:

$$Delay = (k + d) \cdot T_s \; with \; 0 \leq d < 1 \tag{8}$$

As a result, the delay transfer function would be:

$$H_{Delay}(z) = z^{-k} + z^{-d} \tag{9}$$

The fractional exponent cannot be used in the Z domain. So other alternatives shall be used. A common one is using a Thiran filter[13]. These filters have a flat delay for small frequencies, although they loose performance at larger ones, especially near the sampling frequency. The equation that describes the filters is:

$$\begin{cases} H(z) & = \dfrac{a_N z^N + a_{N-1} z^{N-1} + \cdots + a_0}{a_0 z^N + a_1 z^{N-1} + \cdots + a_N} \\ a_j & = (-1)^j \binom{N}{j} \prod_{i=0}^{N} \dfrac{D - N + i}{D - N + j + i} \forall j: 1,2, \ldots, N \\ a_0 & = 1 \\ D & = k + d \\ \binom{N}{j} & = \dfrac{N!}{j!\,(N-j)!} \end{cases} \tag{10}$$

Where the filter order (N) is the upper integer of D, or k+1.

Considering all the different Delay contributions, its value will be between one image sampling period and something over two periods. As a result the degree can be two or three. The Table 1 shows the resulting coefficients, taking intro account the fractional delay.

Table 1. Coefficients of the Thiran Allpass Filter of Order N=1, 2 and 3.

Thiran Filter Order	$\mathbf{a_0}$	$\mathbf{a_1}$	$\mathbf{a_2}$	$\mathbf{a_3}$
k=0, N=1	1	$-\frac{d-1}{d+1}$	-	-
k=1, N=2	1	$-2\frac{d-1}{d+2}$	$\frac{d(d-1)}{(d+2)(d+3)}$	-
k=2, N=3	1	$-3\frac{d-1}{d+3}$	$3\frac{d(d-1)}{(d+3)(d+4)}$	$-\frac{(d+1)d(d-1)}{(d+3)(d+4)(d+5)}$

The next block is the TT Controller. From the model point of view, it can be considered like a DAC converter with an output filter, as shown in Figure 10.

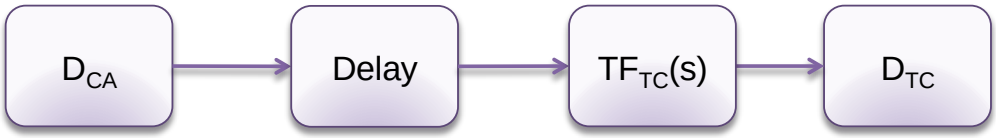

Fig. 10 H_{TC} block diagram.

The Delay is a small fraction of the sampling time, which takes into account the time necessary to process the signal by the DAC and its output. The TF_{TC} is a second order low-pass filter with the same parameters as the TT one, but different values.

$$TF_{TC}(s) = \frac{K_{TC}}{\frac{s^2}{\omega_0^2} + 2\xi\frac{s}{\omega_0} + 1} \qquad (11)$$

The final block diagram is shown in Figure 11.

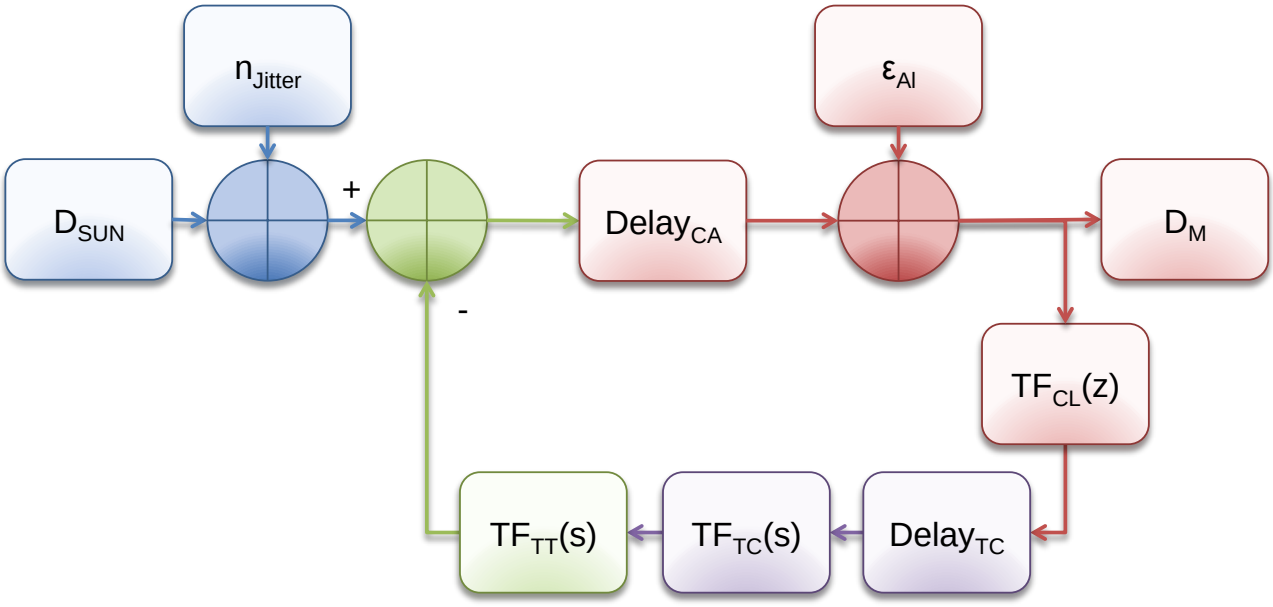

Fig. 11 ISS control loop.

The transfer function can be described by the next formula:

$$D_M = \frac{\left(D_{SUN} + n_{Jitter}\right)Delay_{CA} + \varepsilon_{Al}}{1 + Delay_{CA}TF_{CL}(z)Delay_{TC}TF_{TC}(s)TF_{TT}(s)} \quad (12)$$

3.2 Analyzing the transfer function

The first step is translating the continuous time transfer functions to a discrete one. There are two options to make this transformation, the Zero Order Hold, and the Bilinear one. The first has better matching in the time domain, while the second reflects better the frequency domain. As our requirements are defined in the frequency domain, in concrete at 10Hz frequency, the bilinear transformation is chosen. To improve this matching, a prewarp frequency (f_p) will be used:

$$\begin{cases} s_p = \omega_p \dfrac{z-1}{z+1} \\ \omega_p = \dfrac{2\pi f_p}{tan\left(\dfrac{\pi f_p}{f_s}\right)} \end{cases} \quad (13)$$

This ensures the same behavior at the prewarp frequency. As a result the transfer function becomes:

$$H(z) \equiv \mathcal{Z}\{H(s)\} = H\left(\frac{2\pi f_p}{tan\left(\dfrac{\pi f_p}{f_s}\right)}\frac{z-1}{z+1}\right) \quad (14)$$

Yielding a second order transfer function:

$$\begin{cases} H(s) & = \dfrac{1}{\dfrac{s^2}{\omega_0^2} + 2\xi\dfrac{s}{\omega_0} + 1} \Longrightarrow H(z) = \dfrac{a_2 z^2 + a_1 z + a_0}{b_2 z^2 + b_1 z + b_0} \\ a_0 & = \omega_0^2 \\ a_! & = 2\omega_0^2 \\ a_2 & = \omega_0^2 \\ b_0 & = \omega_0^2 - 2\xi\omega_p\omega_0 + \omega_p^2 \\ b_1 & = 2(\omega_0^2 - \omega_p^2) \\ b_2 & = \omega_0^2 + 2\xi\omega_p\omega_0 + \omega_p^2 \end{cases} \quad (15)$$

The transfer function can be simplified using the prewarp factor (ω_p):

$$\begin{cases} H(s) & = \dfrac{1}{\dfrac{s^2}{\omega_0^2} + 2\xi\dfrac{s}{\omega_0} + 1} \Longrightarrow H(z) = \dfrac{z^2 + 2z + 1}{b_2 z^2 + b_1 z + b_0} \\ b_0 & = 1 - \dfrac{2\xi\omega_p}{\omega_0} + \dfrac{\omega_p^2}{\omega_0^2} \\ b_1 & = 2\left(1 - \dfrac{\omega_p^2}{\omega_0^2}\right) \\ b_2 & = 1 + \dfrac{2\xi\omega_p}{\omega_0} + \dfrac{\omega_p^2}{\omega_0^2} \end{cases} \quad (16)$$

Also, the relationship between the prewarp factor and the resonant frequency can be substituted by a prewarp resonant frequency (ω_0‘):

$$\omega_0' = \frac{\omega_0}{\omega_p} \quad (17)$$

It yields:

$$\begin{cases} H(s) & = \dfrac{1}{\dfrac{s^2}{\omega_0^2} + 2\xi\dfrac{s}{\omega_0} + 1} \Longrightarrow H(z) = \dfrac{z^2 + 2z + 1}{b_2 z^2 + b_1 z + b_0} \\ b_0 & = 1 - \dfrac{2\xi}{\omega_0'} + \dfrac{1}{\omega_0'^2} \\ b_1 & = 2\left(1 - \dfrac{1}{\omega_0'^2}\right) \\ b_2 & = 1 + \dfrac{2\xi}{\omega_0'} + \dfrac{1}{\omega_0'^2} \end{cases} \quad (18)$$

Based on the previous formula, it is possible to translate the different TF inside the formula (12), with the exception of the control loop TF. The delays ($Delay_{CA}$ and $Delay_{TC}$) can be aggregated as the control loop delay ($Delay_{CL}$).

$$\begin{cases} D_M & = \dfrac{(D_{SUN} + n_{Jitter})Delay_{CA} + \varepsilon_{Al}}{1 + Delay_{CL}TF_{CL}(z)TF_{TC}(z)TF_{TT}(z)} \\ Delay_{CL} & = \dfrac{a_{DL3}z^3 + a_{DL2}z^2 + a_{DL1}z + a_{DL0}}{a_{DL0}z^3 + a_{DL1}z^2 + a_{DL2}z + a_{DL3}} \\ TF_{TC}(z) & = K_{TC}\dfrac{z^2 + 2z + 1}{b_{TC2}z^2 + b_{TC1}z + b_{TC0}} \\ TF_{TT}(z) & = K_{TT}\dfrac{z^2 + 2z + 1}{b_{TT2}z^2 + b_{TT1}z + b_{TT0}} \end{cases} \quad (19)$$

The D_M poles define the loop stability, so the analysis will concentrate on the characteristic equation:

$$1 + Delay_{CL}TF_{CL}(z)TF_{TC}(z)TF_{TT}(z) = 0 \quad (20)$$

The equation is difficult to solve analytically due to the large equation degree. For this reason a numerical approximation is done. To make the calculus, the selected prewarp frequency will be 10Hz as it is the one that define the required attenuation ($1/10^{th}$). The expected resonant frequency (ω_0) for the TT it will be over 6rad·kHz. In the TC case, it is expected to be over 60rad·kHz. The ξ usually is below 1 in the TT case, while it is between 1 and 2 in the TC case.

The selected control loop TF is an integrator, as it minimizes the possible offsets, and it is highly stable.

$$TF_{CL}(z) = K_{CL}\frac{1}{1 - z^{-1}} = K_{CL}\frac{z}{z - 1} \quad (21)$$

The different amplification factors (K_{xx}) can be aggregated in one, in the present case, the K_{CL}. Based on these values, the Phase Margin (PM), Gain Margin (GM) and Attenuation (At) at 10Hz hypersurfaces have been calculated.

4. RESULTS

To reach the required attenuation, only the K_{CL} and the $Delay_{CL}$ can be modified. The results show that K_{CL} is the parameter that has major impact on the three figures; while the $Delay_{CL}$ has its major effect on the PM.

The values that allow reaching the required attenuation with a stable characteristic equation are:

- K_{CL}: 1.5
- $Delay_{CL}$: $1.05/f_s$ or 3.5ms

Other requirements are the minimum TT resonant frequency, which must be over 6rad·kHz, and the TT Controller one, which must be at least an order of magnitude higher than the TT one. The Bode plot in Figure 12 shows the Gain Margin (GM) and the Phase Margin (PM).

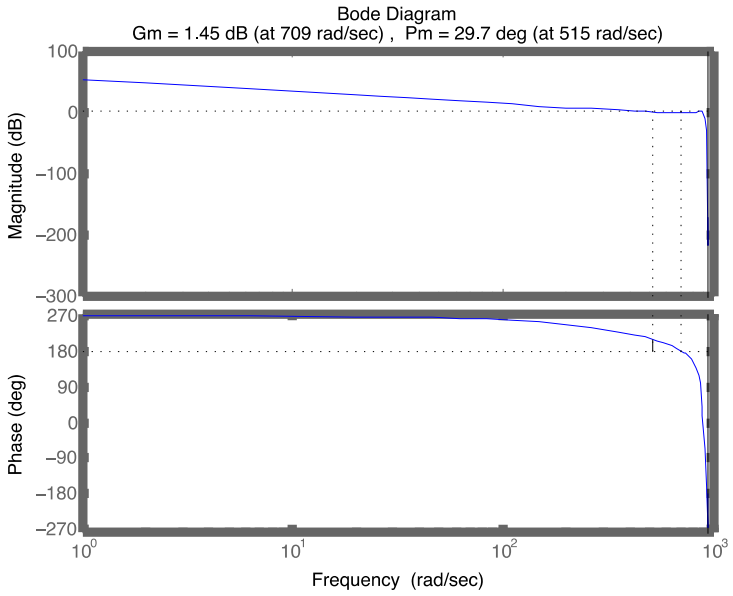

Fig. 12 Transfer function Gain and Phase margins.

The PM is small. It does not reach 30deg, so special care must be taken to minimize the components drifts. The control loop behavior is shown in Figure 13.

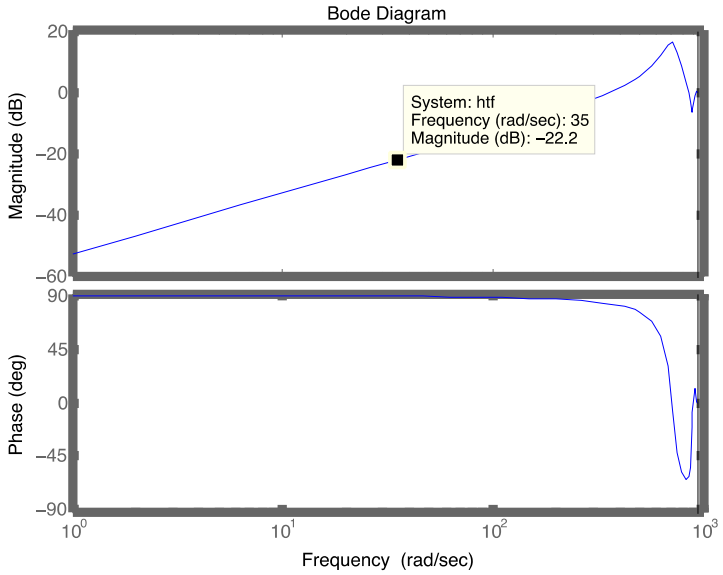

Fig. 13 Control loop Bode diagram.

At a 10Hz (31.4rad·Hz on the figure), the attenuation is 22dB, approximately $1/10^{th}$, which is the system requirement. The margin is small, so special care must be taken to achieve the required parameters values.

The $Delay_{CL}$ imposes a strong requirement on the ISS Control, as it must finish the whole algorithm calculation and transfer the data to the TT Controller in 1.05 frame periods. This implies that the control algorithm calculation must be done while the image is read. The maximum allowed overhead is 167µs. Taking into account the delay introduced by the DAC (21µs), the algorithm can have a maximum overhead of 146µs.

As a result, the parallelization of the ISS Control algorithm is a must, and the image must be properly handled while it is received in order to minimize the delays.

Finally, the algorithm has been analyzed using only a proportional control function, with amplifying factor K_{CL}. This solution works as required, but other alternatives, based on a PID controller are being analyzed, as it could allows improving the phase margin.

5. CONCLUSSIONS

An analysis of stability of the ISS for the SO/PHI instrument has been made. The system includes discrete time and continuous time functions that require a proper transformation between the domains. The resulting equations show that the ISS is feasible, though the phase margin is very small. Also, the allowed overhead for the ISS Control calculations is very small imposing huge restrictions on its architecture. Alternatives based on a PID are being analyzed in order to improve the phase margin.

ACKNOWLEDGMENTS

This work has been funded by the Spanish MINECO through project AYA2012-39636-C06-02, including a percentage from European FEDER funds.

REFERENCES

[1] R. G. Marsden, E. Marsch."Solar Orbiter Science Requirements Document," Issue 2 (2010).
[2] A. Gandorfer, S. K. Solanki, J. Woch, V. Martiınez Pillet, A. Alvarez Herrero and T. Appourchaux, "The Solar Orbiter Mission and its Polarimetric and Helioseismic Imager (SO/PHI)" Journal of Physics: Conference Series 271 (2011)
[3] E. Ballesteros, M. Collados et al., "Two-dimensional, high spatial resolution, solar spectroscopy using a Correlation Tracker. Correlation Tracker description," Astronomy & Astrophisics Supplement series 115, 353-365 (1996).
[4] T. Apporchaux. "The Luminosity Oscillations Imager, a space instrument; from design to science," ESA Publications Division, Noordwiijk, The Nederlands, (2003).
[5] C. Fröhlich. B. N. Andersen. "Virgo: Experiment for helioseismology and solar irradiance monitoring," 1995ESASP.376a.83F (1995).
[6] R. A. Howard. J.D. Moses et al. "Sun Earth Connection Coronal and Heliospheric Investigation (SECCHI)," Springer Space Sci Rev136: 67–115, DOI 10.1007/s11214-008-9341-4 (2008).
[7] T. Shimizu, S. Nagata, S. Tsuneta, et al. "Image Stabilization System for Hinode (Solar-B) Solar Optical Telescope," Springer Science+Business Media B.V. (2007).
[8] "S-340 Piezo Tip / Tilt-Platform", Physik Instrumente (2008)
[9] "NOIS1SM1000A: STAR1000 1M Pixel Radiation Hard CMOS Image Sensor," ON Semiconductor (2012).
[10] "DAC121S101QML: 12-Bit Micro Power Digital-to-Analog Converter with Rail- to-Rail Output," Texas Instruments Incorporated (2012).
[11] "Space-Grade Virtex-4QV Family Overview," Xilinx (2010).
[12] Löfdahl, "Evaluation of image shift measurement algorithms for solar Shack–Hartmann wavefront sensors," Astronomy & Astrophysics, A90, 524 (2010).
[13] Timo I. Laakso, Vesa Välimäki, Matti Karjalainen, and Unto K. Laine, "Splitting the unit delay - tools for fractional delay filter design," IEEE Signal Processing Magazine, vol. 13, no. 1 (1996).